



HAP Code Retreat: Simulating Blazars with a two-zone-hybrid and a spatially resolved SSC model

Stephan Richter
Universität Würzburg



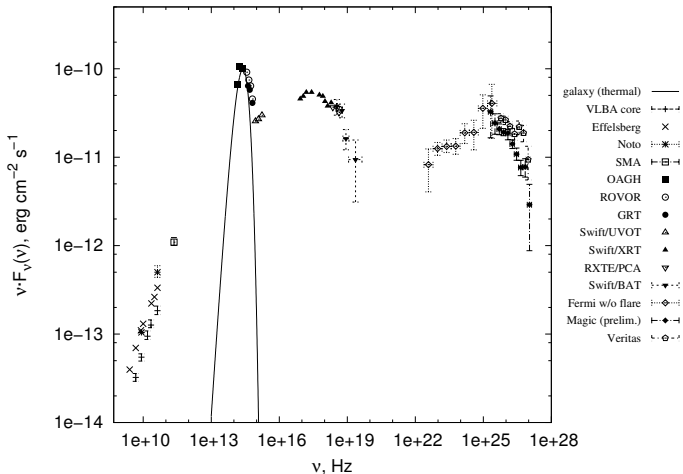
Institut für Theoretische Physik und Astrophysik
May 5, 2020



- ① Two-zone-hybrid model (COJONES)
- ② Spatially resolved SSC model (UNICORN)
 - Motivation
 - Geometry
 - Acceleration
 - Radiation
 - Numerics
 - Results
 - Outlook

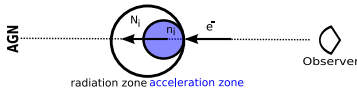
The challenge

Model highly relativistic regions (so called blobs), moving along a jet, accelerating electrons (and possibly protons) to Lorentz factors of $\sim 10^7$, whose radiated spectrum looks approximately like this (example of *Markarian501*):





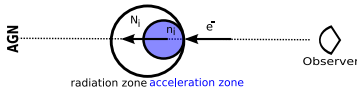
Assume spherical emitting and acceleration region containing isotropic particle distributions and randomly orientated magnetic field in a nested setup:



see Weidinger et al. 2010 for details



Assume spherical emitting and acceleration region containing isotropic particle distributions and randomly orientated magnetic field in a nested setup:

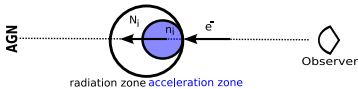


Kinetic equation: acceleration zone

$$\partial_t n_e = \partial_\gamma [(\beta_s \gamma^2 - t_{\text{acc}}^{-1} \gamma) \cdot n_e] + \partial_\gamma [(a+2)t_{\text{acc}}]^{-1} \gamma^2 \partial_\gamma n_e + Q_0 - t_{\text{esc}}^{-1} n_e$$

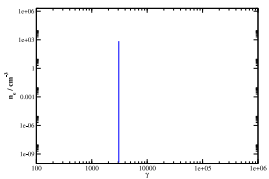
see Weidinger et al. 2010 for details

Assume spherical emitting and acceleration region containing isotropic particle distributions and randomly orientated magnetic field in a nested setup:



Kinetic equation: acceleration zone

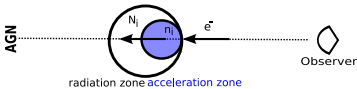
$$\partial_t n_e = \partial_\gamma [(\beta_s \gamma^2 - t_{\text{acc}}^{-1} \gamma) \cdot n_e] + \partial_\gamma [(a+2)t_{\text{acc}}]^{-1} \gamma^2 \partial_\gamma n_e + Q_0 - t_{\text{esc}}^{-1} n_e$$



see Weidinger et al. 2010 for details

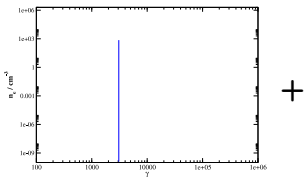


Assume spherical emitting and acceleration region containing isotropic particle distributions and randomly orientated magnetic field in a nested setup:

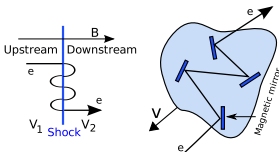


Kinetic equation: acceleration zone

$$\partial_t n_e = \partial_\gamma [(\beta_s \gamma^2 - t_{\text{acc}}^{-1} \gamma) \cdot n_e] + \partial_\gamma [(a+2)t_{\text{acc}}]^{-1} \gamma^2 \partial_\gamma n_e + Q_0 - t_{\text{esc}}^{-1} n_e$$



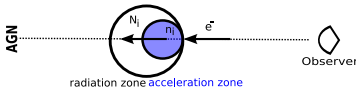
+



see Weidinger et al. 2010 for details

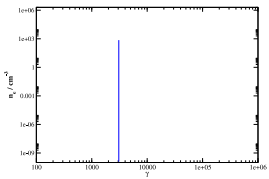


Assume spherical emitting and acceleration region containing isotropic particle distributions and randomly orientated magnetic field in a nested setup:

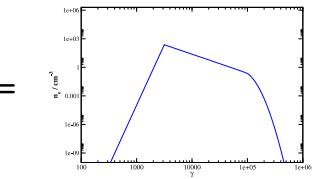
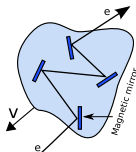
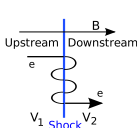


Kinetic equation: acceleration zone

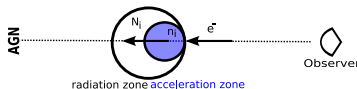
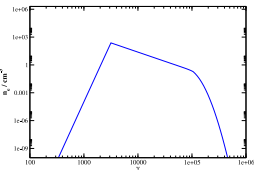
$$\partial_t n_e = \partial_\gamma [(\beta_s \gamma^2 - t_{\text{acc}}^{-1} \gamma) \cdot n_e] + \partial_\gamma [(a+2)t_{\text{acc}}]^{-1} \gamma^2 \partial_\gamma n_e + Q_0 - t_{\text{esc}}^{-1} n_e$$



+

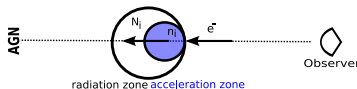
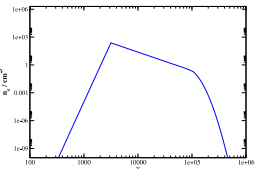


see Weidinger et al. 2010 for details



Kinetic equation: radiation zone

$$\partial_t N_e = \partial_\gamma [(\beta_s \gamma^2 + \dot{\gamma}_{IC}) \cdot N_e] + b^3 t_{\text{esc}}^{-1} n_e - t_{\text{esc},N}^{-1} N_e$$



Kinetic equation: radiation zone

$$\partial_t N_e = \partial_\gamma [(\beta_s \gamma^2 + \dot{\gamma}_{IC}) \cdot N_e] + b^3 t_{esc}^{-1} n_e - t_{esc,N}^{-1} N_e$$

Photon distribution

$$\partial_t N_{ph} = R_{syn} + R_{IC} - c \alpha_{SSA} N_{ph} - t_{esc,ph}^{-1} N_{ph}$$

Selfconsistent SSC limit
see Weidinger and Spanier 2010 for details

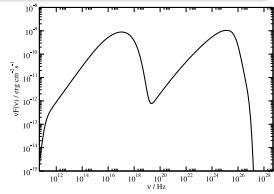
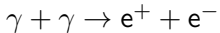




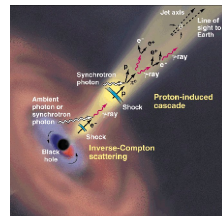
Photo-Meson production:

- $p + \gamma \rightarrow p + n_0\pi^0 + n_+\pi^+ + n_-\pi^-$
- $\pi^\pm \rightarrow \mu^\pm + \nu_\mu/\bar{\nu}_\mu$
- $\pi^0 \rightarrow \gamma + \gamma$
- $\mu^\pm \rightarrow e^\pm + \nu_e/\bar{\nu}_e + \bar{\nu}_\mu/\nu_\mu$

Resulting γ -radiation above $\approx 10^{28}$ Hz will be opaque to



\Rightarrow pair induced cascades and cascade radiation will emerge in jets with non-thermal p^+ present¹.





Now there are 4 **non-linear coupled** equations in the radiation zone:

Kinetic equations: radiation zone

$$\begin{aligned}\partial_t N_{p^+} &= \partial_\gamma [\beta_p \gamma^2 \cdot N_{p^+}] + b^3 t_{\text{esc},p}^{-1} n_{p^+} - t_{\text{esc},p,N}^{-1} N_{p^+} \\ \partial_t N_{e^-} &= \partial_\gamma [(\beta_e \gamma^2 + \dot{\gamma}_{\text{IC}}) \cdot N_{e^-}] + b^3 t_{\text{esc},e}^{-1} n_{e^-} + Q_{pp} + Q_{p\gamma^-} - t_{\text{esc},e,N}^{-1} N_{e^-} \\ \partial_t N_{e^+} &= \partial_\gamma [(\beta_e \gamma^2 + \dot{\gamma}_{\text{IC}}) \cdot N_{e^+}] + Q_{pp} + Q_{p\gamma^+} - t_{\text{esc},e,N}^{-1} N_{e^+}\end{aligned}$$

Photon distribution

$$\partial_t N_{\text{ph}} = R_{\text{syn}} + R_{\text{IC}} + R_{\pi^0} - c (\alpha_{\text{SSA}} + \alpha_{\text{pp}}) N_{\text{ph}} - t_{\text{esc,ph}}^{-1} N_{\text{ph}}$$



Now there are 4 **non-linear coupled** equations in the radiation zone:

Kinetic equations: radiation zone

$$\begin{aligned}\partial_t N_{p^+} &= \partial_\gamma [\beta_p \gamma^2 \cdot N_{p^+}] + b^3 t_{\text{esc}, p}^{-1} n_{p^+} - t_{\text{esc}, p, N}^{-1} N_{p^+} \\ \partial_t N_{e^-} &= \partial_\gamma [(\beta_e \gamma^2 + \dot{\gamma}_{\text{IC}}) \cdot N_{e^-}] + b^3 t_{\text{esc}, e}^{-1} n_{e^-} + Q_{pp} + Q_{p\gamma^-} - t_{\text{esc}, e, N}^{-1} N_{e^-} \\ \partial_t N_{e^+} &= \partial_\gamma [(\beta_e \gamma^2 + \dot{\gamma}_{\text{IC}}) \cdot N_{e^+}] + Q_{pp} + Q_{p\gamma^+} - t_{\text{esc}, e, N}^{-1} N_{e^+}\end{aligned}$$

Photon distribution

$$\partial_t N_{\text{ph}} = R_{\text{syn}} + R_{\text{IC}} + R_{\pi^0} - c (\alpha_{\text{SSA}} + \alpha_{\text{pp}}) N_{\text{ph}} - t_{\text{esc, ph}}^{-1} N_{\text{ph}}$$

- Kelner Aharonian parameterization of the SOPHIA Monte Carlo results is used to calculate $Q_{p\gamma^-}$, $Q_{p\gamma^+}$, $R_{\pi^0} \Rightarrow$ unstable intermediates (π^\pm, π^0, μ^\pm) are not taken into account



Now there are 4 **non-linear coupled** equations in the radiation zone:

Kinetic equations: radiation zone

$$\begin{aligned}\partial_t N_{p^+} &= \partial_\gamma [\beta_p \gamma^2 \cdot N_{p^+}] + b^3 t_{\text{esc}, p}^{-1} n_{p^+} - t_{\text{esc}, p, N}^{-1} N_{p^+} \\ \partial_t N_{e^-} &= \partial_\gamma [(\beta_e \gamma^2 + \dot{\gamma}_{\text{IC}}) \cdot N_{e^-}] + b^3 t_{\text{esc}, e}^{-1} n_{e^-} + Q_{pp} + Q_{p\gamma^-} - t_{\text{esc}, e, N}^{-1} N_{e^-} \\ \partial_t N_{e^+} &= \partial_\gamma [(\beta_e \gamma^2 + \dot{\gamma}_{\text{IC}}) \cdot N_{e^+}] + Q_{pp} + Q_{p\gamma^+} - t_{\text{esc}, e, N}^{-1} N_{e^+}\end{aligned}$$

Photon distribution

$$\partial_t N_{\text{ph}} = R_{\text{syn}} + R_{\text{IC}} + R_{\pi^0} - c (\alpha_{\text{SSA}} + \alpha_{\text{pp}}) N_{\text{ph}} - t_{\text{esc, ph}}^{-1} N_{\text{ph}}$$

- Kelner Aharonian parameterization of the SOPHIA Monte Carlo results is used to calculate $Q_{p\gamma^-}$, $Q_{p\gamma^+}$, $R_{\pi^0} \Rightarrow$ unstable intermediates (π^\pm, π^0, μ^\pm) are not taken into account
- Cascades will emerge in the optically thick regime $> 10^{28}$ Hz



A spatially resolved model - UNICORN



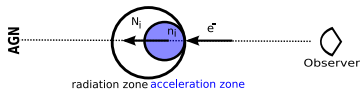
- acceleration due to Fermi I happens at finite size shock
 $\Rightarrow R_{acc} \ll R_{rad}$
- acceleration efficiency should depend on distance to shock
- for energies with $t_{cool} < lct$ the blob simply isn't homogenous \Rightarrow effect on global spectral energy density (SED)



- acceleration due to Fermi I happens at finite size shock
 $\Rightarrow R_{acc} \ll R_{rad}$
- acceleration efficiency should depend on distance to shock
- for energies with $t_{cool} < lct$ the blob simply isn't homogenous \Rightarrow effect on global spectral energy density (SED)
- compute *multiple shock*-scenarios
- homogenous models constrain time variability to $\Delta t > R_{rad}/c$ \Rightarrow inhomogenous models allow shorter timescales while preserving causality



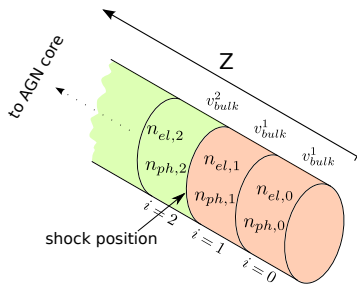
- acceleration due to Fermi I happens at finite size shock
 $\Rightarrow R_{acc} \ll R_{rad}$
- acceleration efficiency should depend on distance to shock
- for energies with $t_{cool} < lct$ the blob simply isn't homogenous \Rightarrow effect on global spectral energy density (SED)
- compute *multiple shock*-scenarios
- homogenous models constrain time variability to $\Delta t > R_{rad}/c$ \Rightarrow inhomogenous models allow shorter timescales while preserving causality
- time lags might be explained by light travel time between different components of the blob
- cooling and reacceleration of intermediates of e.g. photohadronic processes can be treated in detail



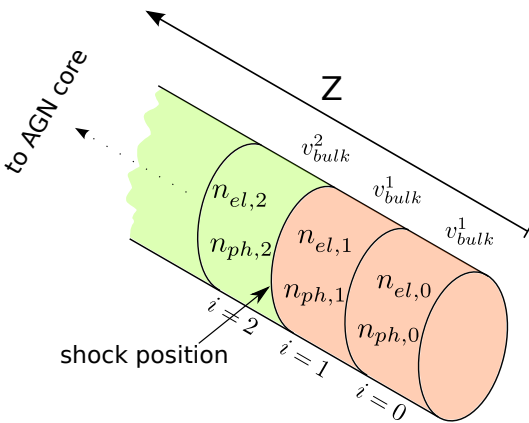
expand two-zone-model
to N-zone-model

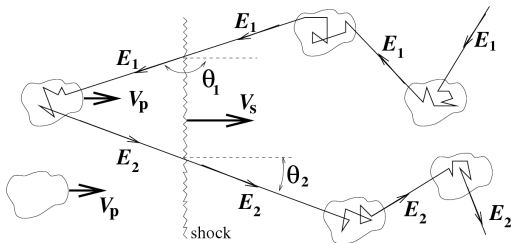


move from nested to
aligned setup

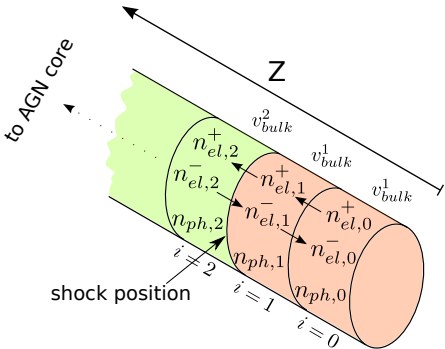


- devide simulation region into N slices in the direction parallel to shock normal
- each slice has local bulk speed, electron density, photon density (, magnetic field, radius)

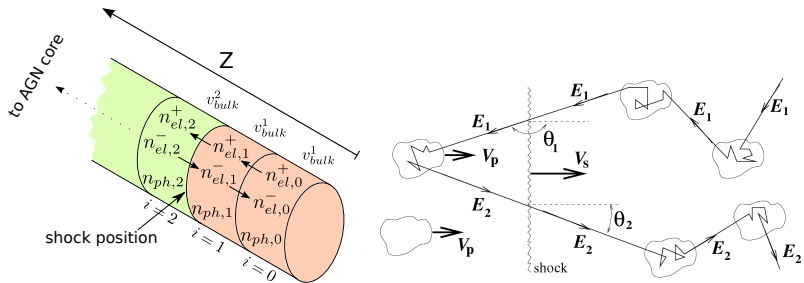




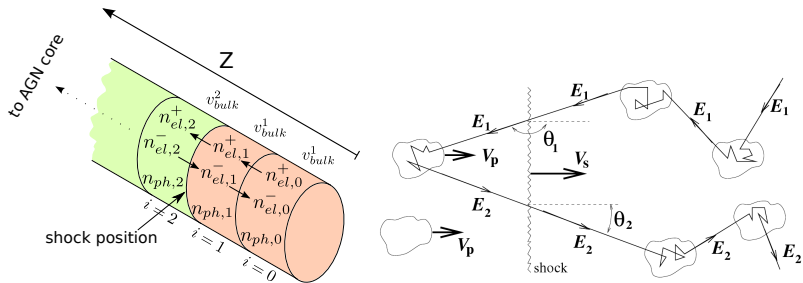
- multiple scattering on both sides of a shock
- scattering is elastic in plasma frame
- when particles cross the shock, the boost into the bulk frame distorts the isotropy of the target distribution
- hence head on collisions are more likely and acceleration becomes more efficient



- split electron population into two half spheres; one moving downstream (n^+), the other moving upstream (n^-)
- connecting the slices via advection of electrons between them
- shock is represented by jump in bulk velocity u between neighboured zones



- in shock frame: $v_{bulk}^1 = u_u = -V_S$, $v_{bulk}^2 = u_d = V_P - V_S$, $R = \frac{u_u}{u_d}$
- relativistic treatment yields $V_P = \frac{V_S(R-1)}{R-V_S^2}$



- in shock frame: $v_{bulk}^1 = u_u = -V_S$, $v_{bulk}^2 = u_d = V_P - V_S$, $R = \frac{u_u}{u_d}$
- relativistic treatment yields $V_P = \frac{V_S(R-1)}{R-V_S^2}$
- scattering is controlled via the probability for an electron to change its propagation direction (including the boost into the new frame of reference)



- stochastic acceleration independent of presence of shock
- repeated scattering of relativistic particles leads to acceleration second order in bulk velocity
- included in model as diffusion in momentum space



- stochastic acceleration independent of presence of shock
- repeated scattering of relativistic particles leads to acceleration second order in bulk velocity
- included in model as diffusion in momentum space

Fermi-II acceleration included in kinetic equation

$$\frac{\partial F}{\partial t} = \frac{1}{p^2} \frac{\partial}{\partial p} \left[p^2 \cdot \left(\langle \dot{p}_{FII} \rangle \frac{\partial F}{\partial p} + \dot{p}_{cool} \cdot F \right) \right] + S(x, p, t)$$

$$\text{with } \langle \dot{p}_{FII} \rangle = p^2 \frac{V_A^2}{9\kappa_{||}} = p^2 D$$

V_A ... Alfvén velocity; $\kappa_{||}$... parallel diffusion coefficient



time evolution of photon density

$$\frac{\partial N}{\partial t} = -c \cdot \kappa_{\nu, \text{SSA}} \cdot N + \frac{4\pi}{h\nu} \cdot (\epsilon_{\nu, \text{IC}} + \epsilon_{\nu, \text{sync}})$$

- $\kappa_{\nu, \text{SSA}}$ - Synchrotron Self Absorption coefficient
 - calculated using the Melrose Approximation
- $\epsilon_{\nu, \text{IC}}$ - changes due to invers compton scattering
 - full integration of photon and electron density using the Klein-Nishina cross section
- $\epsilon_{\nu, \text{sync}}$ - yields due to synchrotron radiation
 - integration of electron density using the Melrose approximation for a single electron spectrum

see Richter and Spanier 2012 for details



- update shock properties

electrons

- calculate the change in electron density for each slice due to convection from/to neighbouring regions and the source function
- compute backreaction of photon density (inverse compton) on electrons
- integrate the Vlasov-Equation in momentum space in each slice
- perform scattering of electrons from one half-space into the other due to pitch angle scattering

photons

- compute synchrotron power
- calculate synchrotron self absorption
- compute inverse compton gains and losses
- update photon density



numerical costs:

- due to statistical approach to Fermi I higher γ_{max} , hence smaller dt
- compute inverse compton scattering in each slice
 $\Rightarrow \mathcal{O}(N_z \cdot N_\nu \cdot (N_\gamma N_\nu))$



numerical costs:

- due to statistical approach to Fermi I higher γ_{max} , hence smaller dt
- compute inverse compton scattering in each slice
 $\Rightarrow \mathcal{O}(N_z \cdot N_\nu \cdot (N_\gamma N_\nu))$

\Rightarrow calculate double integrals on GPUs via *OpenCL*



numerical costs:

- due to statistical approach to Fermi I higher γ_{max} , hence smaller dt
- compute inverse compton scattering in each slice
 $\Rightarrow \mathcal{O}(N_z \cdot N_\nu \cdot (N_\gamma N_\nu))$

\Rightarrow calculate double integrals on GPUs via *OpenCL*

CPU

GPU



numerical costs:

- due to statistical approach to Fermi I higher γ_{max} , hence smaller dt
- compute inverse compton scattering in each slice
 $\Rightarrow \mathcal{O}(N_z \cdot N_\nu \cdot (N_\gamma N_\nu))$

\Rightarrow calculate double integrals on GPUs via *OpenCL*

CPU

update shock

GPU



numerical costs:

- due to statistical approach to Fermi I higher γ_{max} , hence smaller dt
- compute inverse compton scattering in each slice
 $\Rightarrow \mathcal{O}(N_z \cdot N_\nu \cdot (N_\gamma N_\nu))$

\Rightarrow calculate double integrals on GPUs via *OpenCL*

CPU

update shock

update electrons

GPU

inverse compton scattering



numerical costs:

- due to statistical approach to Fermi I higher γ_{max} , hence smaller dt
- compute inverse compton scattering in each slice
 $\Rightarrow \mathcal{O}(N_z \cdot N_\nu \cdot (N_\gamma N_\nu))$

\Rightarrow calculate double integrals on GPUs via *OpenCL*

CPU

update shock

update electrons

GPU

inverse compton scattering





numerical costs:

- due to statistical approach to Fermi I higher γ_{max} , hence smaller dt
- compute inverse compton scattering in each slice
 $\Rightarrow \mathcal{O}(N_z \cdot N_\nu \cdot (N_\gamma N_\nu))$

\Rightarrow calculate double integrals on GPUs via *OpenCL*

CPU

update shock

update electrons

update photons

GPU

inverse compton scattering



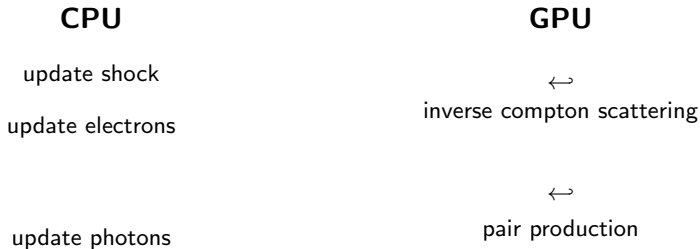
pair production



numerical costs:

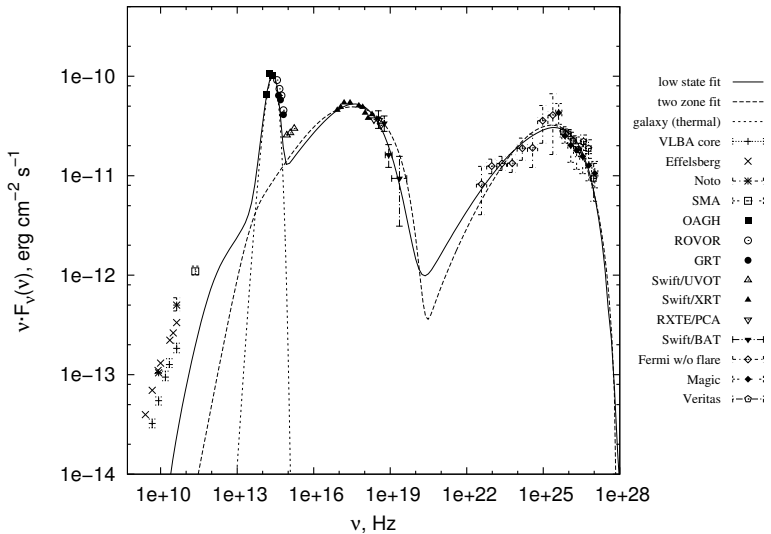
- due to statistical approach to Fermi I higher γ_{max} , hence smaller dt
- compute inverse compton scattering in each slice
 $\Rightarrow \mathcal{O}(N_z \cdot N_\nu \cdot (N_\gamma N_\nu))$

\Rightarrow calculate double integrals on GPUs via *OpenCL*





Results





synchrotron self absorption by a powerlaw distribution

equivalence of brightness and kinetic temperature leads to a flux

$$F_\nu \propto \nu^{\frac{5}{2}}$$

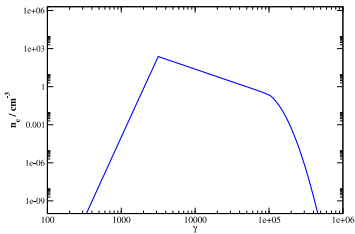


synchrotron self absorption by a powerlaw distribution

equivalence of brightness and kinetic temperature leads to a flux

$$F_\nu \propto \nu^{\frac{5}{2}}$$

usual approach:
increase γ_{min} or γ_{inject} , respectively



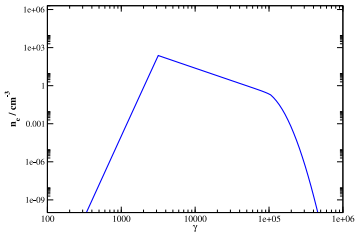


synchrotron self absorption by a powerlaw distribution

equivalence of brightness and kinetic temperature leads to a flux

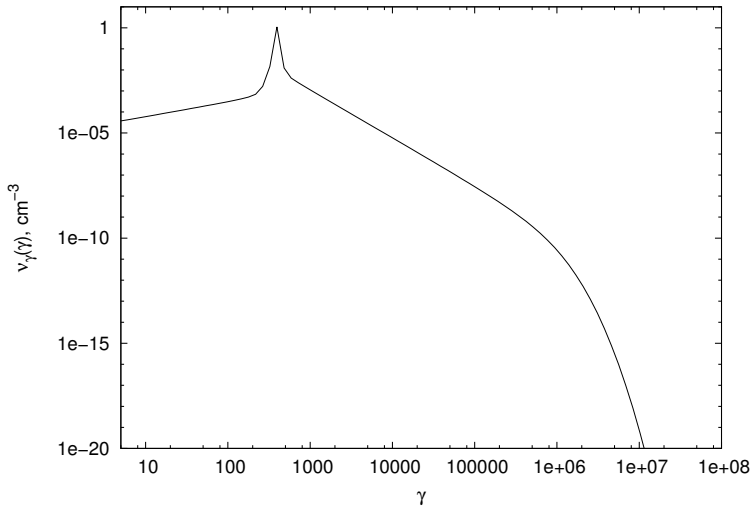
$$F_\nu \propto \nu^{\frac{5}{2}}$$

usual approach:
increase γ_{min} or γ_{inject} , respectively

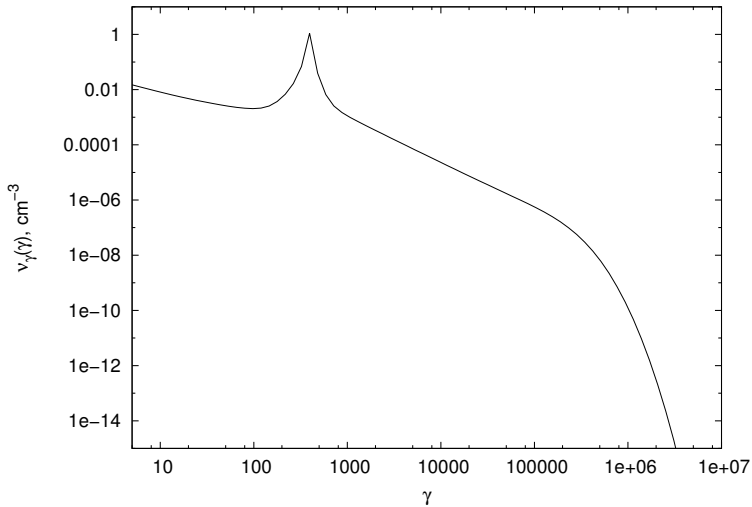


synchrotron radiation of a single electron

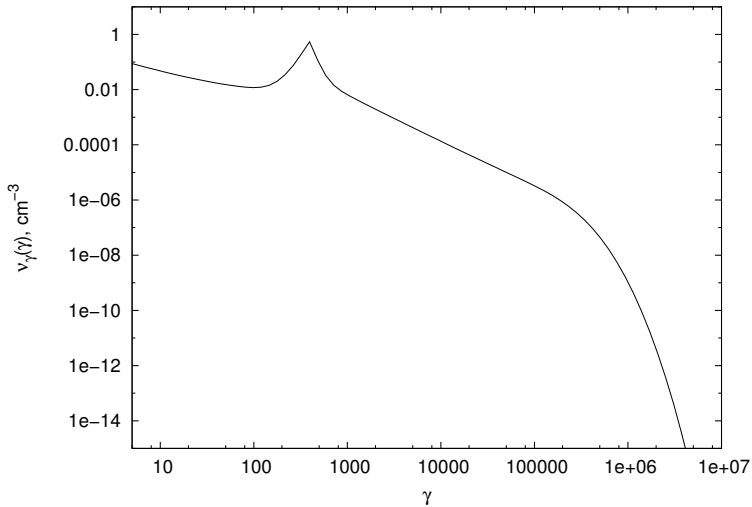
$$P_\nu(\gamma, \nu) = \frac{\sqrt{3} q^3 B}{m c^2} \cdot \frac{\nu}{\nu_c} \int_{\frac{\nu}{\nu_c}}^{\infty} d\eta \ K_{\frac{5}{3}}(\eta) \stackrel{\text{small } \nu}{\propto} \nu^{\frac{1}{3}}$$



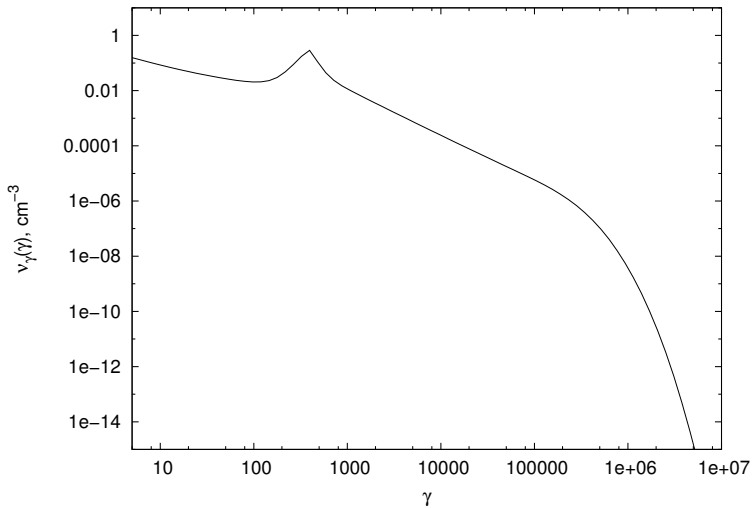
Electron distribution at different distances to the shock.



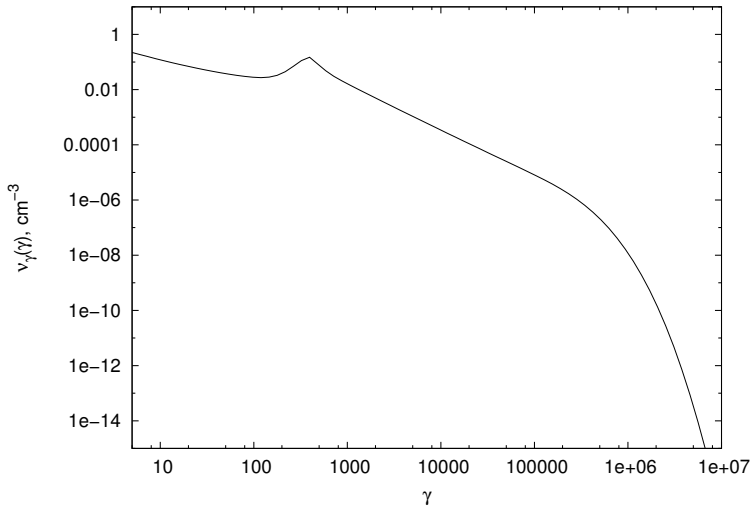
Electron distribution at different distances to the shock.



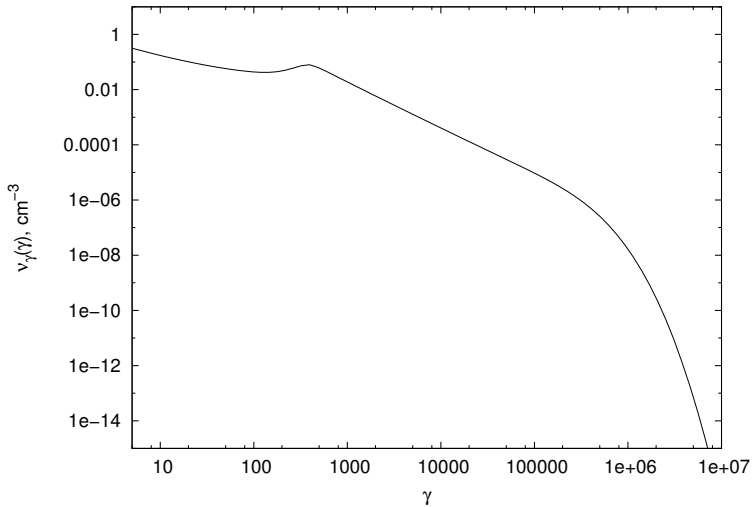
Electron distribution at different distances to the shock.



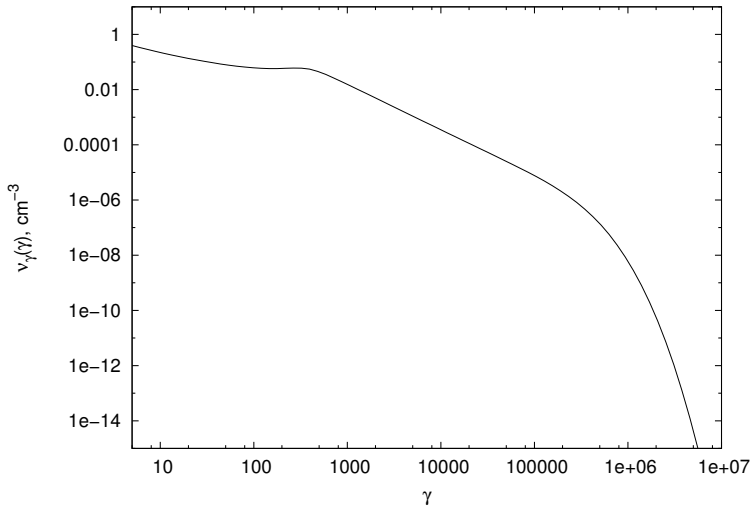
Electron distribution at different distances to the shock.



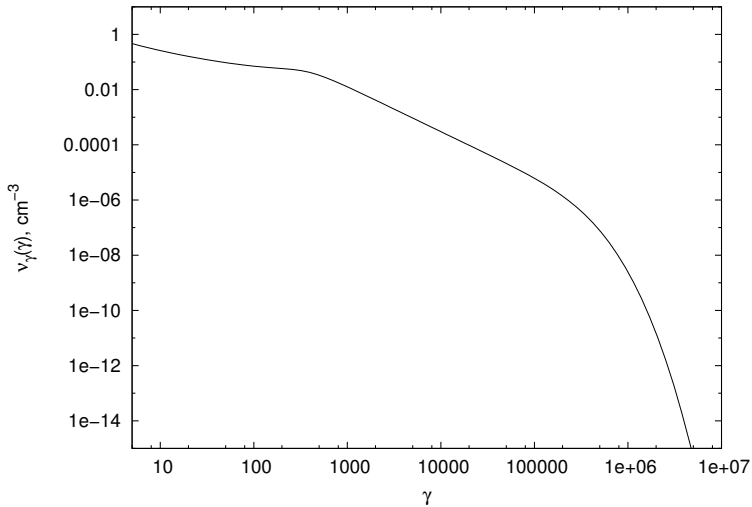
Electron distribution at different distances to the shock.



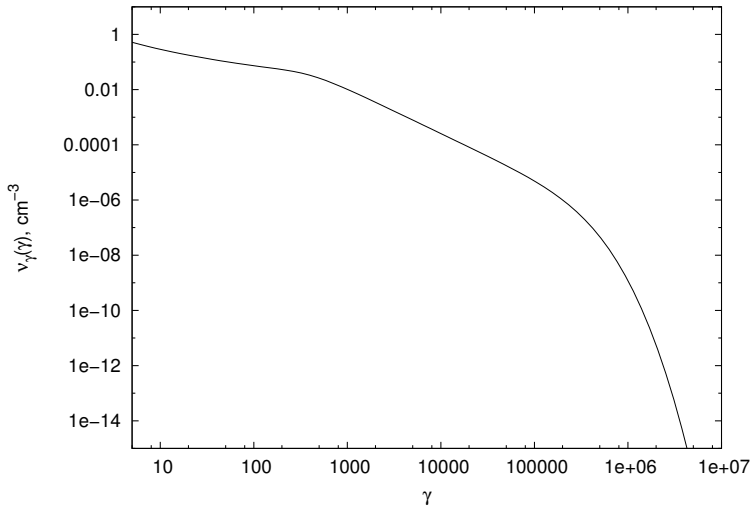
Electron distribution at different distances to the shock.



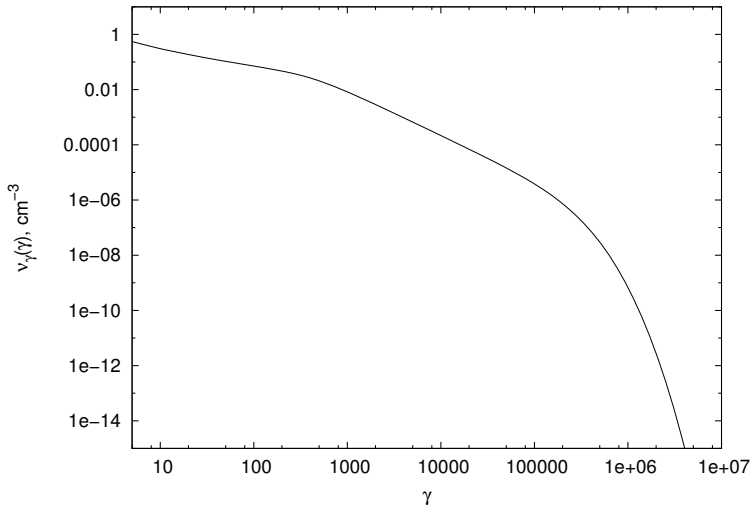
Electron distribution at different distances to the shock.



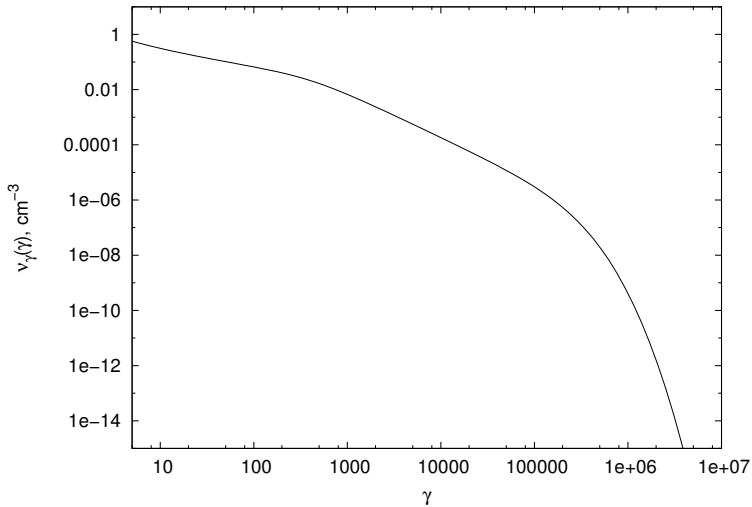
Electron distribution at different distances to the shock.



Electron distribution at different distances to the shock.

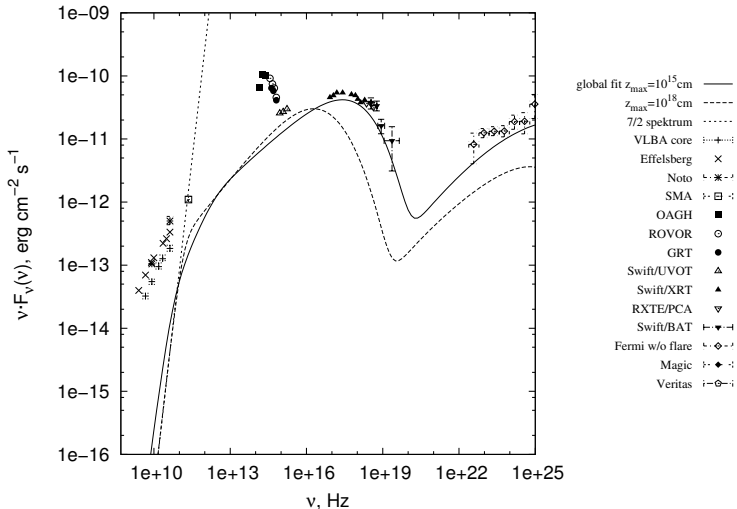


Electron distribution at different distances to the shock.



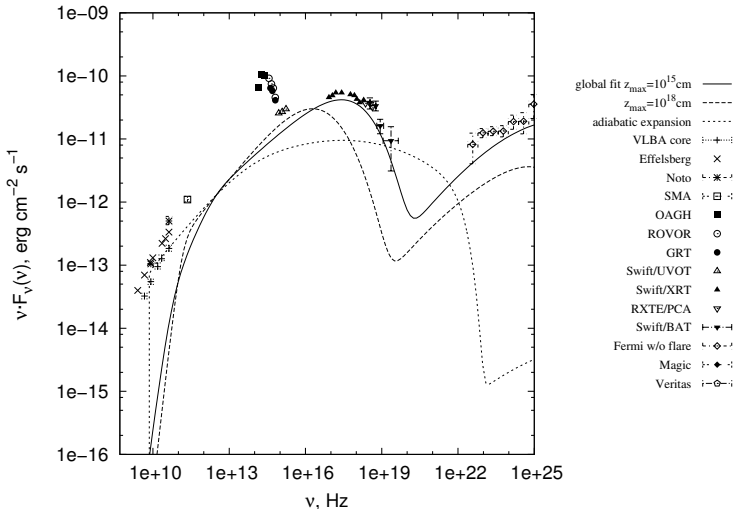
Electron distribution at different distances to the shock.

Radio spectrum

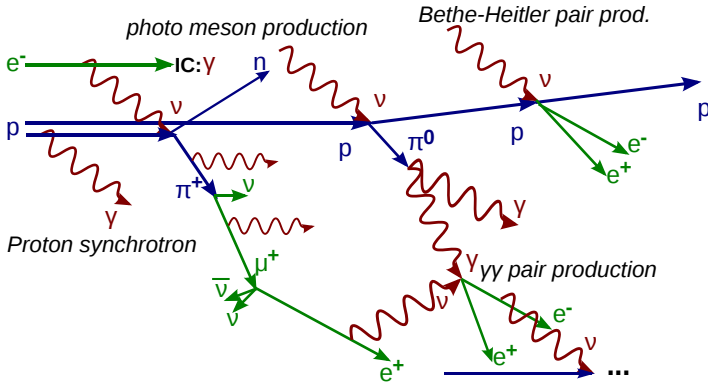


Effect of significant larger simulation region.

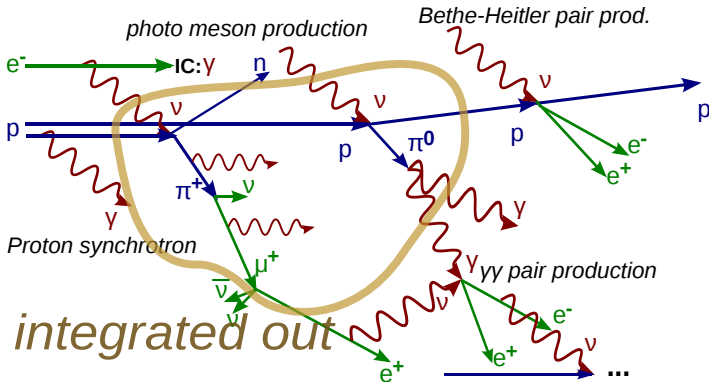
Adiabatic expansion



Effect of additional adiabatic expansion.

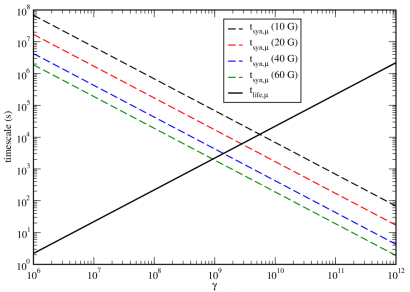


schematic of the dominant photohadronic processes [from: Weidinger 2012]



schematic of the dominant photohadronic processes [from: Weidinger 2012]

- cooling (and possibly acceleration) of intermediates is relevant in AGNs
- \Rightarrow using model by Hümmer et al. 2010
- How does this influence resulting SEDs and variation timescales?
- calculation of realistic, flavour splitted neutrino spectra



Muon lifetime vs. dominant cooling process [from: Weidinger 2012]



- self consistent spatially resolved SSC model
- addition of photohadronics (in progress)
- although higher numerical costs, reasonable computation times thanks to GPGPU
- access to radio information via adiabatic expansion
- investigate cooling and reacceleration effects on hadronic modelling
- also: time variability, morphology (especially magnetic fields)

spatial resolution brings new opportunities, but new problems, too



Thank you



- S. Hümmer, M. Rüger, F. Spanier, and W. Winter. Simplified Models for Photohadronic Interactions in Cosmic Accelerators. *Astrophys. J.*, 721: 630–652, Sept. 2010. doi: 10.1088/0004-637X/721/1/630.
- S. Richter and F. Spanier. A Spatially Resolved SSC Shock-In-Jet Model. *International Journal of Modern Physics Conference Series*, 8:392, 2012. doi: 10.1142/S2010194512004977.
- M. Weidinger and F. Spanier. Modeling the Emission from Blazar Jets:.. the Case of PKS 2155-304. *International Journal of Modern Physics D*, 19: 887–892, 2010. doi: 10.1142/S0218271810017159.
- M. Weidinger, M. Rüger, and F. Spanier. Modelling the steady state spectral energy distribution of the BL-Lac Object PKS 2155-30.4 using a selfconsistent SSC model. *Astrophysics and Space Sciences Transactions*, 6: 1–7, Jan. 2010. doi: 10.5194/astra-6-1-2010.



calculations over several orders of magnitudes in Lorentz factor γ and photon energy $\nu \Rightarrow$



calculations over several orders of magnitudes in Lorentz factor γ and photon energy $\nu \Rightarrow$

use logarithmic grids

- choose N_γ , $i \in [0, N_\gamma - 1]$
- fraction of neighbouring grid points $\delta_\gamma = \frac{\gamma_{i+1}}{\gamma_i} = \left(\frac{\gamma_{max}}{\gamma_{min}} \right)^{\frac{1}{N_\gamma-1}}$
- get grid points via $\gamma_i = \gamma_{min} \cdot \delta_\gamma^i$
- cell interfaces $\gamma_i^{interface} = \gamma_{i-1/2} = \gamma_{min} \cdot \delta_\gamma^{(i-\frac{1}{2})} = \sqrt{\gamma_{i-1} \cdot \gamma_i}$
- cell size $\gamma_i^{interval\ size} = \gamma_{i+1}^{interface} - \gamma_i^{interface}$



calculations over several orders of magnitudes in Lorentz factor γ and photon energy $\nu \Rightarrow$

use logarithmic grids

- choose N_γ , $i \in [0, N_\gamma - 1]$
- fraction of neighbouring grid points $\delta_\gamma = \frac{\gamma_{i+1}}{\gamma_i} = \left(\frac{\gamma_{\max}}{\gamma_{\min}}\right)^{\frac{1}{N_\gamma-1}}$
- get grid points via $\gamma_i = \gamma_{\min} \cdot \delta_\gamma^i$
- cell interfaces $\gamma_i^{interface} = \gamma_{i-1/2} = \gamma_{\min} \cdot \delta_\gamma^{(i-\frac{1}{2})} = \sqrt{\gamma_{i-1} \cdot \gamma_i}$
- cell size $\gamma_i^{interval\ size} = \gamma_{i+1}^{interface} - \gamma_i^{interface}$

integrations are performed via second order *simpson's rule*, generalised for log-grids